

Point-contact spectroscopy on tunable constrictions in GaAs

T. Bever, A. D. Wieck, K. v. Klitzing, and K. Ploog

Max-Planck-Institut für Festkörperforschung, Heisenbergstrasse 1, D-7000 Stuttgart 80, Federal Republic of Germany

P. Wyder

Max-Planck-Institut für Festkörperforschung, Hochfeld-Magnetlabor, 25 Avenue des Martyrs,

F-38042 Grenoble CEDEX, France

(Received 17 May 1991)

In quasi-one-dimensional channels formed in the two-dimensional electron gas of an $\text{Al}_x\text{Ga}_{1-x}\text{As}/\text{GaAs}$ heterostructure, the second derivative d^2V/dI^2 of the voltage-current characteristic is measured at low temperatures as a function of the voltage drop V over the channel length. In increasing the lateral confinement, strong resonant structures appear at voltages V that correspond to energies of GaAs phonon density-of-states maxima for acoustical as well as optical phonons. Compared with metal point-contact spectroscopy, this technique offers reproducible tunability of buried point contacts.

Recently, quantum point contacts were prepared and characterized,^{1,2} leading to the discovery of quantized conductance of these quasi-one-dimensional (1D) channels in multiples of $2e^2/h$. These systems were induced via split gates on top of $\text{Al}_x\text{Ga}_{1-x}\text{As}-\text{GaAs}$ heterostructures with high electron mobilities. Another way of creating a 1D confining potential was found by fabricating in-plane-gated quantum wires by means of Ga^+ focused ion beam (FIB) implantation,³ a method which has the advantage of maskless writing on as-grown heterostructures. In both cases the quantized steps in the point-contact resistance were measured with an applied source-drain voltage of less than 1 mV. Quantization breakdown occurs if the applied voltage reaches a certain critical value which is of the order of the 1D subband spacing (typically 2–4 meV).⁴ Hot electron effects have been extensively investigated in lateral tunneling experiments^{5,7} and electroluminescence studies,⁸ showing emission of optical phonons by the electrons. Very recently, the kinetic energies of injected electrons from quantum point contacts have been measured.⁹

In this paper we present an analysis of the current-voltage characteristic of quantum point contacts for source-drain voltages up to 100 mV. All devices discussed in the following were fabricated by means of FIB implantation. This kind of point-contact spectroscopy has been performed previously on metals¹⁰ and metal-semiconductor junctions¹¹ in order to study the electron-phonon interaction function α^2F (Eliashberg function) from an analysis of the d^2V/dI^2 characteristic in the limit of contact dimensions small compared to the effective mean free path l_e .¹² Roughly speaking, the Eliashberg function α^2F is the product of the phonon density of states F and the squared matrix element α for the electron-phonon interaction averaged over the Fermi sphere. For three-dimensional electron systems this has been calculated by solving the full linear Boltzmann equation for the point-contact problem.^{13,14} Unfortunately no such theoretical work has yet been done in the case of a two-dimensional electron gas (2DEG). In the following we will show that the second derivative

d^2V/dI^2 of a point contact in a 2DEG reflects structures in the phonon density of states (DOS). Historically, the fundamental work on 1D channels^{1,2} was initially motivated by this spectroscopic application leading to its designation as “semiconductor point contact” by Van Wees *et al.*¹ and Kouwenhoven *et al.*⁴

Samples were prepared from a $\text{GaAs}/\text{Al}_{0.3}\text{Ga}_{0.7}\text{As}$ heterostructure (grown by molecular beam epitaxy) with carrier density $n = 2.1 \times 10^{11} \text{ cm}^{-2}$ and a zero-field mobility of $\mu = 3.0 \times 10^5 \text{ cm}^2/\text{Vs}$ at $T = 4 \text{ K}$. This corresponds to a transport mean free path of $2.5 \mu\text{m}$ and a Fermi energy $E_F = 7.2 \text{ meV}$ for an effective mass of $m = 0.07m_e$ (m_e , free electron mass). The as-grown samples are mesa etched with standard optical lithography to define a $150\text{-}\mu\text{m}$ -wide Hall bar with $150\text{-}\mu\text{m}$ spaced $50\text{-}\mu\text{m}$ -wide potential probes. By means of focused Ga^+ -ion beam insulation writing with a spot diameter of 100 nm and a dose of $1.3 \times 10^{13} \text{ cm}^{-2}$ we create an in-plane-gate.³ In combination with an insulating line written from the sample edge close to the gate this gives a tunable constriction (Fig. 1). We denote the shortest distance across the constriction between the center points of the FIB-exposed spots the geometrical width which is $w_{\text{geo}} = 2 \mu\text{m}$. By applying different gate voltages to terminal 6 in Fig. 1 with respect to the source (terminal 5) both the effective width and the carrier concentration of the constriction can be increased (positive gate voltage) or decreased (negative gate voltage), respectively. The effective channel width w can be tuned down to zero by a negative gate voltage V_g . In the measurements presented here pinchoff occurs at threshold voltages of typically $V_{\text{th}} = -3 \text{ V}$. The leakage current between gate and source and/or drain is well below 100 pA for $-5 < V_g < +5 \text{ V}$. For more details see Ref. 3.

The measurements are performed in a bath cryostat at 4.2 K. The drain-source bias V is obtained by passing a constant dc current I through the device. We measure the differential resistance dV/dI with standard lock-in technique by superimposing a 10-nA ac current of frequency 86 Hz. This ac current is large enough to give a reasonable signal-to-noise ratio and small enough to

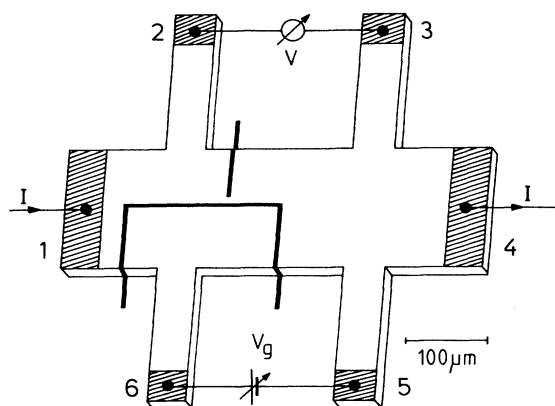


FIG. 1. Sketch of the sample. The focused ion beam written path is indicated by the bold lines.

probe only a small voltage interval ($< 1\ \text{mV}$) around the applied bias. Driving the current through contacts 1 and 4 we measure both the differential resistance and the bias voltage using contacts 2 and 3 in a four-terminal arrangement. The second derivative d^2V/dI^2 is obtained numerically from the experimental dV/dI data.

Figure 2 shows the I - V characteristics of the constric-

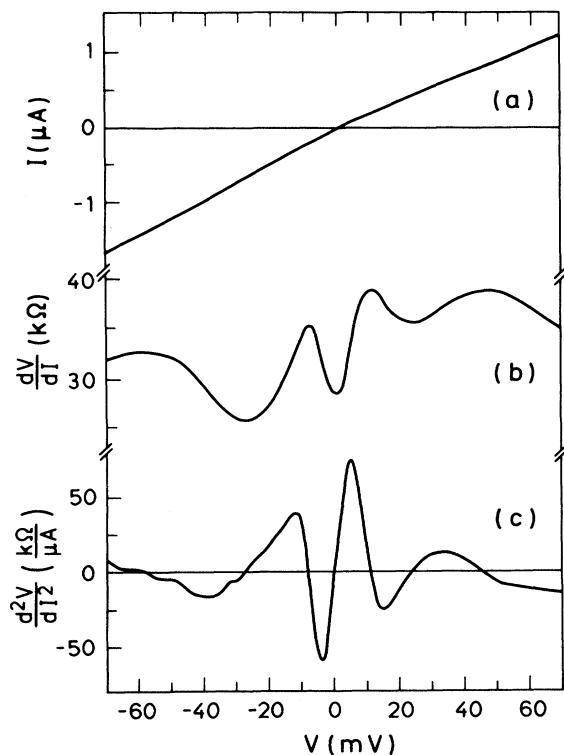


FIG. 2. (a) Current-voltage (I - V) characteristics, (b) the first, and (c) the second derivative of V with respect to I . The applied gate voltage is $V_g = -1.0\ \text{V}$.

tion with an applied gate voltage $V_g = -1.0\ \text{V}$ [2(a)], the first derivative dV/dI [2(b)], and the second derivative d^2V/dI^2 [2(c)], respectively.

In Fig. 3 we present the measured differential resistance of a second sample for different gate voltages as a function of the applied bias voltage. The lowest curve ($V_g = +4.0\ \text{V}$) shows almost perfect Ohmic behavior. In tuning the gate voltage to negative values the zero bias resistance is increased monotonically. This increase is accompanied by a pronounced peak around zero bias for $V_g \leq -2.2\ \text{V}$. This peak is consistent with the interpretation that near pinch-off a potential barrier is built up in the constriction leading to higher resistance. A finite bias V over the channel length is needed to overcome this barrier and, as a consequence, the resistance drops rapidly.¹⁵

For negative gate voltages large deviations from Ohmic behavior are observed in both current directions at a bias voltage of $V \approx 8\ \text{mV}$. An additional nonlinearity around

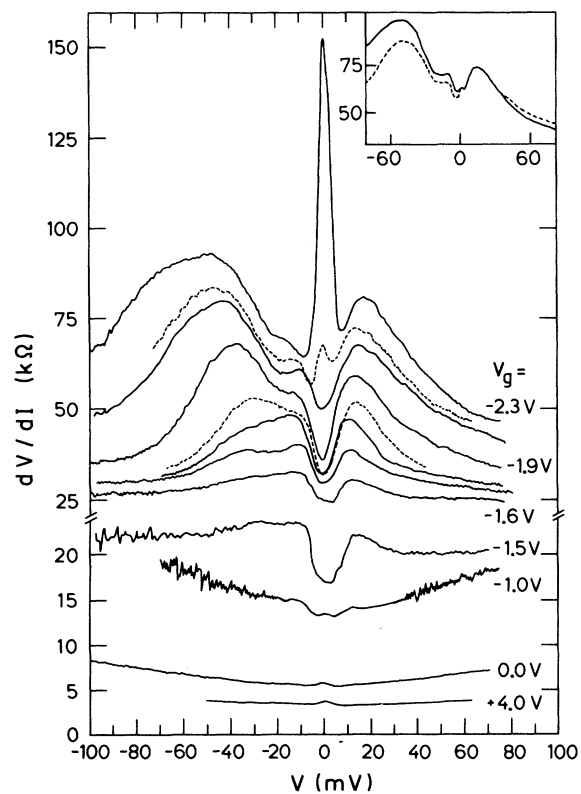


FIG. 3. Differential resistance measured in the contact configuration of Fig. 1 as a function of the bias voltage for gate voltages $V_g = 4.0, 0.0, -1.0, -1.5, -1.6, -1.7, -1.75, -1.8, -1.9, -2.1, -2.2, \text{ and } -2.3\ \text{V}$ for the lowest to the uppermost curve, respectively. The curves for $V_g = -2.2$ and $-1.8\ \text{V}$ cross adjacent curves and are thus dashed for clarity. The inset curves for $V_g = -2.15\ \text{V}$, the dashed curve measured in the same contact configuration as the data in the main figure. The solid curve is recorded with V_g applied relative to contact 2 instead of contact 5 in the main figure (see Fig. 1). The axis labeling of the inset refers to the lettering of the main figure.

$V \approx 32$ mV arises with increasing strength when V_g is tuned to even smaller values. In the case of Fig. 3 this high-energy nonlinearity is seen only in the current direction from terminal 4 to 1 whereas in the case of Fig. 2(b) both the high- and the low-energy nonlinearities are observed in the positive and in the negative current direction. We attribute the asymmetry in Fig. 3 to microscopic properties of the sample used for Fig. 3. To check the influence of the voltage drop V on the gate potential (so-called pinch off behavior) we show in the inset of Fig. 3 curves measured with the gate voltage applied to one and the other end of the channel. The curves are very similar and exhibit the same resonant structures exactly at the same voltages. Thus, we can definitely exclude the possibility that resonant structures in the curves are due to changes in the confining potential.

In Fig. 4 we show the second derivative d^2V/dI^2 as a

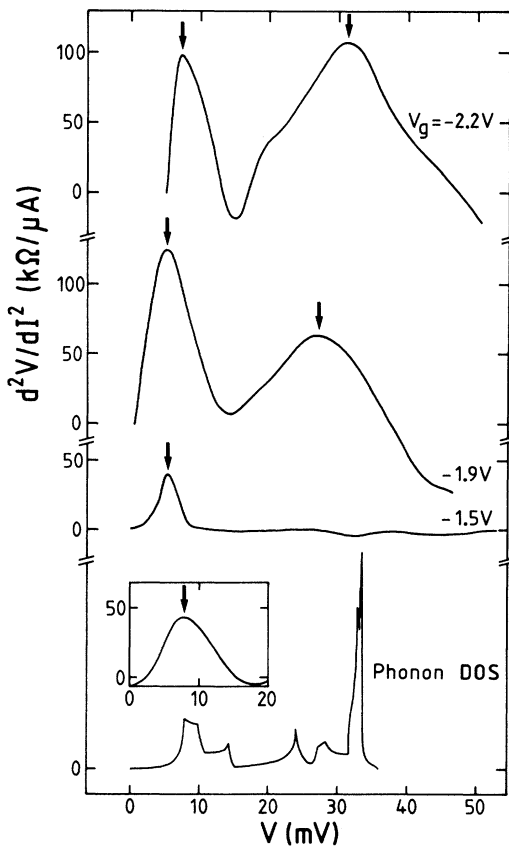


FIG. 4. Second derivative of the voltage-current characteristics of the constriction for gate voltages V_g as indicated in the figure, the Fermi energy of the 2DEG adjacent to the constriction being $E_F = 7.2$ meV. The curve in the inset is obtained for a sample with higher Fermi energy $E_F = 16.5$ meV, gate voltage $V_g = -3.95$ V, and geometrical width $w_{\text{geo}} = 1.5$ μm . This higher negative gate voltage is needed for the higher carrier density n and scales with n and $1/w_{\text{geo}}$, respectively. The axis scales of the inset refer to the lettering of the main figure. The lowest curve in the figure represents the energy dependence of the phonon DOS of GaAs in arbitrary units on the vertical scale (Ref. 16).

function of the bias for different gate voltages with the current flow in the negative direction (terminal 4 to 1). The nonlinearities at low energy and high energy appear as positive peaks in d^2V/dI^2 as indicated by arrows in Fig. 4, already visible in Fig. 2(c) as minima for negative bias and maxima for positive bias, respectively. At the bottom of Fig. 4 we have plotted the calculated phonon DOS of GaAs (Ref. 16) for purposes of comparison. The marked structures in the second derivative are very close to maxima in the phonon DOS. This strongly indicates that d^2V/dI^2 is a measure of the energy dependence of the electron-phonon interaction as in the case of point-contact spectroscopy on metals, thereby reflecting the phonon DOS.

In order to rule out the possibility that the Fermi energy of the 2DEG ($E_F = 7.2$ meV) might affect the position of the low-energy peak we have prepared samples in the same way as the samples discussed above but from an $\text{Al}_x\text{Ga}_{1-x}\text{As}/\text{GaAs}$ heterostructure with carrier density $n = 4.8 \times 10^{11} \text{ cm}^{-2}$ which yields a Fermi energy $E_F = 16.5$ meV. As can be seen from Fig. 4 there is no shift in the position of the peak even though the Fermi energy differs by more than a factor of 2. In total, seven samples prepared from three different wafers have been investigated, all showing resonant structures at the same energy positions.

In contrast to conventional point-contact spectroscopy the width of the constriction can be tuned continuously via the in-plane-gate in our samples. This gives us the possibility to adjust different ratios w/l_e . It is very instructive to see in Fig. 3 how the features become more prominent as the width is decreased via the applied gate voltage. Since in point-contact spectroscopy the condition $w < l_e$ must hold, we expect resonances which become more pronounced the smaller w is, in consistence with the observed phenomena.

Another advantage of this method is due to the fact that the current does not flow through a free surface as is the case in a metal point contact¹² since in our samples the point contact is formed within the 2DEG. Thus spectra of the same constriction are well reproduced even after warming up the sample or exposing it to air.

Since the 2DEG is located at the $\text{Al}_x\text{Ga}_{1-x}\text{As}/\text{GaAs}$ interface we expect contributions from the $\text{Al}_x\text{Ga}_{1-x}\text{As}$ phonon DOS to the spectrum. It has been shown^{17,18} that the GaAs-like LO phonon in $\text{Al}_x\text{Ga}_{1-x}\text{As}$ is shifted to lower energy ($\Delta E \approx -1.5$ meV for $x = 0.3$). Therefore the corresponding peak value in d^2V/dI^2 is expected to move towards the low-energy side. This is consistent with our observation that the maxima in d^2V/dI^2 occur at voltages slightly below the value expected from the phonon DOS in GaAs.

Other scattering processes such as those with charged impurities also contribute to the point-contact spectra. The interaction with charged impurities leads to increasing scattering times for higher electron energies because the Rutherford cross section decreases dramatically as the velocity of the electrons increases. This may explain the drop in differential resistance in the regime of medium bias voltage. For a full discussion of the system, intersubband scattering and scattering due to the interface

roughness must also be considered.

We would like to point out that the spectra presented in Figs. 2–4 contain a wealth of information which may serve to characterize devices like FIB written quasi-1D channels rugged enough to study higher voltage effects as shown here. So far a detailed theoretical analysis to give a more profound quantitative understanding of the data is not available.

Finally it is worth noting that the noise in the measurements shown in Fig. 3 reaches a maximum level for a gate voltage $V_g \approx -1.0$ V and decreases again with increasing negative gate voltage, which is a reproducible effect. An interpretation for this effect has been given in terms of circuit instabilities caused by the occurrence of negative differential resistance in a 1D channel.^{19,20}

In conclusion we have reported on detailed measurements of the differential resistance of a buried constric-

tion carrying over the concept of point-contact spectroscopy to the field of semiconductor physics. Our results indicate that the second derivative of the I - V characteristic of a 1D channel connecting two 2DEG's provides a direct measurement of the 2D electron-phonon coupling $\alpha^2 F$. With an in-plane-gate we are able to tune the width of the constriction continuously from 2D to 1D which makes it possible to study the effect of the ratio w/l_e on the spectra. Point-contact spectroscopy on 2D electron systems promises to be a useful tool to study the phonon DOS in semiconductors especially for those materials for which neutron-diffraction data cannot be obtained because of the lack of volume crystals (e.g., $\text{Al}_x\text{Ga}_{1-x}\text{As}$).

We gratefully acknowledge financial support of the Bundesministerium für Forschung und Technologie of the Federal Republic of Germany.

-
- ¹B. J. van Wees, H. van Houten, C. W. J. Beenakker, J. G. Williamson, L. P. Kouwenhoven, D. van der Marel, and C. T. Foxon, *Phys. Rev. Lett.* **60**, 848 (1988).
- ²D. A. Wharam, T. J. Thornton, R. Newbury, M. Pepper, H. Ahmed, J. E. F. Frost, D. G. Hasko, D. C. Peacock, D. A. Ritchie, and G. A. C. Jones, *J. Phys. C* **21**, L209 (1988).
- ³A. D. Wieck and K. Ploog, *Appl. Phys. Lett.* **56**, 928 (1990).
- ⁴L. P. Kouwenhoven, B. J. van Wees, C. J. P. M. Harmans, J. G. Williamson, H. van Houten, C. W. J. Beenakker, C. T. Foxon, and J. J. Harris, *Phys. Rev. B* **39**, 8040 (1989).
- ⁵C. P. Umbach, A. Palevski, M. Heiblum, and U. Sivan, *J. Vac. Sci. Technol. B* **7**, 2003 (1989).
- ⁶A. Palevski, C. P. Umbach, and M. Heiblum, *Appl. Phys. Lett.* **55**, 1421 (1989).
- ⁷U. Sivan, M. Heiblum, and C. P. Umbach, *Phys. Rev. Lett.* **63**, 992 (1989).
- ⁸C. L. Petersen, M. R. Frei, and S. A. Lyon, *Phys. Rev. Lett.* **63**, 2849 (1989).
- ⁹J. G. Williamson, H. van Houten, C. W. J. Beenakker, M. E. I. Broekaart, L. I. A. Spendeler, B. J. van Wees, and C. T. Foxon, *Phys. Rev. B* **41**, 1207 (1990).
- ¹⁰I. K. Yanson, *Zh. Eksp. Teor. Fiz.* **66**, 1035 (1974) [*Sov. Phys.—JETP* **39**, 506 (1974)].
- ¹¹M. Pepper, *J. Phys. C* **13**, L709 (1980); **13**, L717 (1980); **13**, L721 (1980).
- ¹²A. M. Duif, A. G. M. Jansen, and P. Wyder, *J. Phys. Condens. Matter* **1**, 3157 (1989), and references therein.
- ¹³I. O. Kulik, R. I. Shekhter, and A. N. Omelyanchouk, *Solid State Commun.* **23**, 301 (1977).
- ¹⁴A. P. van Gelder, *Solid State Commun.* **35**, 19 (1980).
- ¹⁵T. Bever, A. D. Wieck, K. v. Klitzing, and K. Ploog, *Phys. Rev. B* **44**, 3424 (1991).
- ¹⁶G. Dolling and R. A. Cowley, *Proc. Phys. Soc. London* **88**, 463 (1963).
- ¹⁷N. Saint-Cricq, G. Landa, J. B. Renucci, I. Hardy, and A. Muñoz-Yague, *J. Appl. Phys.* **61**, 1206 (1987).
- ¹⁸S. Baroni, S. de Gironcoli, and P. Giannozzi, *Phys. Rev. Lett.* **65**, 84 (1990).
- ¹⁹R. J. Brown, M. J. Kelly, M. Pepper, H. Ahmed, D. G. Hasko, D. C. Peacock, J. E. F. Frost, D. A. Ritchie, and G. A. C. Jones, *J. Phys. Condens. Matter* **1**, 6285 (1989).
- ²⁰M. J. Kelly, R. J. Brown, C. G. Smith, D. A. Wharam, M. Pepper, H. Ahmed, D. G. Hasko, D. C. Peacock, J. E. F. Frost, R. Newbury, D. A. Ritchie, and G. A. C. Jones, *Electron. Lett.* **25**, 992 (1989).